

Origin of the diastereofacial selectivity in the nucleophilic addition to chiral acyclic ketones. An *ab initio* MO study

Osamu Takahashi,^{*a} Ko Saito,^a Yuji Kohno,^b Hiroko Suezawa,^{*c} Shinji Ishihara^c and Motohiro Nishio^{*d}

^a Department of Chemistry, Graduate School of Science, Hiroshima University, Kagamiyama, Higashi-Hiroshima 739-8526, Japan. E-mail: shu@hiroshima-u.ac.jp

^b Shock Wave Research Center, Institute of Fluid Science, Tohoku University, 2-1-1 Katahira, Aoba-ku, Sendai 980-8577, Japan

^c Instrumental Analysis Center, Yokohama National University, Hodogaya-ku, Yokohama 240-8501, Japan. E-mail: suezawa@ynu.ac.jp

^d The CHPI Institute, 3-10-7 Narusedai, Machida, Tokyo 194-0043, Japan. E-mail: dionisio@tim.hi-ho.ne.jp

Received (in Montpellier, France) 22nd August 2003, Accepted 13th October 2003

First published as an Advance Article on the web 6th February 2004

Ab initio MO calculations were carried out, at the MP2/6-311G(d,p)//MP2/6-31G(d) level, to investigate the conformational Gibbs energy of alkyl 1-phenylethyl ketones, $C_6H_5CHCH_3COR$, **1** ($R = CH_3$, C_2H_5 , $i-C_3H_7$, $t-C_4H_9$). Rotamers **a** and **a'** whereby R is synclinal to C_6H_5 and the benzylic methyl group is nearly eclipsed to $C=O$ have been shown to be the most stable in every case. Rotamer **a** is stabilized by a 5-member CH/π hydrogen bond and is more abundant than **a'**, which is stabilized by a less effective 6-member CH/π bond. The diastereomeric ratio of the product secondary alcohols in the nucleophilic addition to **1** was estimated on the basis of the ground-state rotamer distribution. The Gibbs energy of the diastereomeric transition states was also calculated for a model reaction ($C_6H_5CHCH_3COR + LiH$) at the same level of approximation. The transition-state geometries leading to the predominant product are similar to those of the ground-state conformation. In geometries leading to the minor product, the relevant torsion angles are twisted to avoid unfavourable steric interactions. The short CH/π and CH/O distances suggest that these weak hydrogen bonds are operating in stabilizing the transition structures. The above two methods gave results consistent with each other. The mechanism of 1,2-asymmetric induction can thus be explained on the basis of the simple premise that the geometry of the transition state resembles the ground-state conformation of the substrate and the nucleophilic reagent approaches from the less hindered side of the carbonyl π -face.

Introduction

A half-century has elapsed since an empirical rule was proposed for the stereoselective addition of nucleophiles to chiral carbonyl compounds.¹ This is known as Cram's rule and various models have since appeared to predict the sense of the π -facial selectivity and the product ratio of the 1,2-asymmetric induction. These include the Cram chelate model,¹ the Cram open-chain model,¹ the Cornforth dipolar model,² the Felkin model³ and the Karabatsos model.⁴ Of these, the stereochemical mechanism is well-elucidated for the chelate and dipolar models, and the predictive power of the stereoselectivity is satisfactory. This is because the above two models are founded on sound physicochemical bases that the conformation of the reactants is more or less fixed by the chelation^{1,5} or dipole-dipole interaction² between polar groups.

On the contrary, the underlying concept has not been well-understood for the other three models, which deal with typical acyclic carbonyl compounds. In other words, the influence of the chiral atom in acyclic compounds on a nearby reaction centre within the same molecule remains one of the most important but yet unexplained issues in stereochemistry.^{6,7} The origin of the π -facial diastereoselectivity includes various factors such as steric, conformational,⁸ electrostatic⁹ and anisotropic inductive effects.¹⁰ Herein we present our

interpretation of the mechanism of 1,2-asymmetric induction of acyclic carbonyl compounds, on the grounds of the rotamer distribution calculated by the *ab initio* MO method. Calculations were also carried out for the transition states of a model reaction ($C_6H_5CHCH_3COR + LiH$). We will show that the above two methods give the same conclusion, which is that the transition state of the reaction is reactant-like and the conformational effect is most important for the π -facial diastereoselectivity.

Computational method

The Gaussian 98 program¹¹ was used. Electron correlation energies were calculated by applying the second order Møller–Plesset (MP2) perturbation theory. The geometry of the reactants and transition states was optimized at the MP2/6-31G(d) level of approximation. Using these geometries, single point calculations were performed at the MP2/6-311G(d,p) level to estimate the energies of the conformers. Vibrational frequencies were calculated using the analytical second derivatives at the same level as the geometry optimization for each conformer. We verified that there is only one imaginary frequency for each transition state. Using these results, the thermal energy corrections were added to the total Gibbs energy at 298.15 K and 1 atmosphere of pressure.

Results and discussion

Conformational Gibbs energy of alkyl 1-phenylethyl ketones

The conformational energy of alkyl 1-phenylethyl ketones $C_6H_5CHCH_3COR$, **1** ($R = CH_3, C_2H_5, i-C_3H_7, t-C_4H_9$), was reported in a previous paper.¹² Fig. 1 is the rotational energy profile of **1** with $R = CH_3$ at the MP2/6-31(d) level. Rotamer **a** whereby R is synclinal to C_6H_5 (R/C_6H_5 torsion angle ϕ of 77°) and antiperiplanar to the benzylic methyl group (Me) has been found to be the most stable. A second well is noted at $\Phi = -77^\circ$ (rotamer **b**) accompanied with a shallow minimum at -45° . In these geometries CH/π interactions are able to operate.^{13,14} The dearth of the rotamer corresponding to the R/C_6H_5 antiperiplanar geometry¹⁵ (CO/C_6H_5 eclipsed) is impressive; only an unclear shoulder is found at ϕ ca. 150° . This is consistent with our earlier NMR data.¹⁶ We think this is a consequence of unfavourable electrostatic interactions between the $C=O$ dipole and the quadrupole of C_6H_5 .

Here we calculated the conformational Gibbs energy by adding the thermal energy corrections to the total energy at 298.15 K and 1 atmosphere of pressure. Table 1 summarizes the Gibbs energies of the rotamers.¹⁷ Rotamer **a** is more stable than rotamer **b** by 2.13–2.51 kcal mol⁻¹ for the methyl and 5.25 kcal mol⁻¹ for the *t*-butyl homologue. The stability of rotamers **a** and **a'** (*vide infra*) is understood since only in these geometries can the CH/O hydrogen bonds^{18–20} between the benzylic methyl group and carbonyl oxygen exist (CH_3/CO torsion angle ψ around $16–25^\circ$ for **a** and $34–40^\circ$ for **a'**). Unfavourable steric effects (R vs. CH_3) may enhance the relative instability of rotamer **b**.†

In the ethyl and isopropyl homologues, three energy minima (two types: **a** and **a'**) were found about the rotation of the $C(=O)-C\alpha$ bond. The more stable **a** bears an $\alpha-CH$ pointing toward C_{ipso} , thus forming a 5-member CH/π bond, while rotamer **a'** bears a 6-member CH/π bond ($\beta-CH$ interacting with C_6H_5). This is consistent with the notion that a 5-member hydrogen bond is more favourable than a 6-membered one.²¹ Table 2 summarizes the rotameric abundance. The population of rotamer **a** is 95.9% when $R = CH_3$ and gradually decreases to 94.3% and 90.2%, respectively, for $R = C_2H_5$ and $i-C_3H_7$. The population of rotamer **a'** increases in the same order; the *t*-butyl homologue exists only in geometry **a'**.

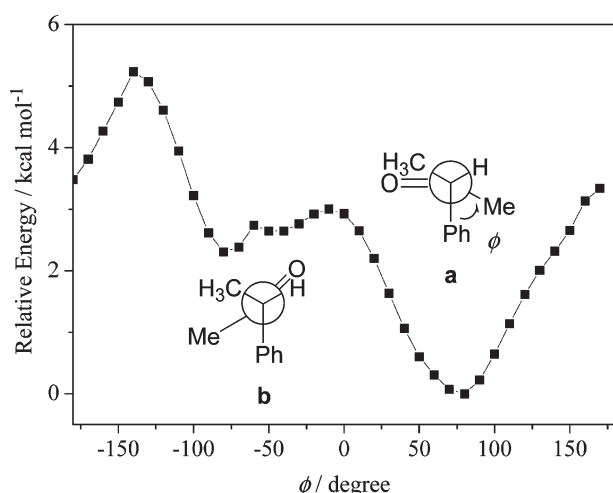


Fig. 1 Rotational energy profile of **1** with $R = CH_3$ at the MP2/6-31(d) level.

† We find no reasonable explanation for the presence of rotamer **b** corresponding to the shallow well at $\phi = -45^\circ$

Table 1 Relative Gibbs energy (kcal mol⁻¹) at 298.15 K and 1 atmosphere of pressure at the MP2/6-311G(d,p)/MP2/6-31G(d) level of approximation. In parentheses is given the C_6H_5-C-R torsion angle ϕ . In brackets is the number of atoms forming the intramolecular CH/π bond

R	Rotamers a , a'	Rotamers b , b'
CH_3	0.00 (77) [5] a	2.51 (–45) [5] b 2.13 (–77) [5] b
C_2H_5	0.00 (79) [5] a 1.05 (77) [5] a 2.05 (93) [6] a'	2.30 (–40) [5] b 2.57 (–78) [5] b 3.26 (–78) [6] b'
$i-C_3H_7$	0.00 (71) [5] a 1.55 (96) [6] a' 2.30 (92) [6] a'	2.45 (–63) [5] b 4.91 (–90) [6] b' 7.50 (–75) [6] b'
$t-C_4H_9$	0.00 (93) [6] a'	5.25 (–71) [6] b'

Stereochemical course of the nucleophilic addition to alkyl 1-phenylethyl ketones

With regard to the hypotheses dealing with nucleophilic addition to acyclic carbonyl compounds, the most popular are models proposed by Cram,¹ Felkin³ and Karabatsos.⁴ Cram's open-chain model [Fig. 2(a)] assumes that group L (L: largest, M: medium, S: smallest) is antiperiplanar to the allegedly bulky $C=O$ group. According to this model, the major product results from the preferential attack of a nucleophile on the side of the group labelled S. Karabatsos presented another hypothesis on the ground of NMR spin-coupling data of aliphatic aldehydes.²² In this model, M or L is nearly eclipsed to the carbonyl group. According to Karabatsos, the configuration of the major product can be predicted by considering the equilibrium of the two conformations [Fig. 2(b)].

Felkin and associates postulated that L is orthogonal to the carbonyl group. According to their suggestion, the approach of the nucleophile to the reactant is expected to be anti to L, thus avoiding unfavourable steric interactions [Fig. 2(c)]. This model is consistent with much experimental data and has been supported by a number of theoretical studies.^{8,9,23} In most cases the above three models predict the correct configuration of the preferred product; however, they fail to predict (or say nothing about) the product ratio.

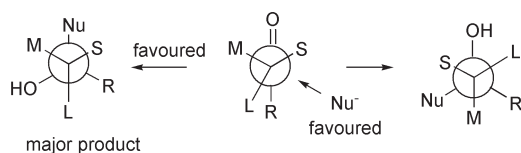
Previously we reported on the mechanism of oxidation of sulfides to sulfoxide diastereomers.²⁴ The experimental data²⁵ was reproduced by assuming that the geometry of the transition state is reactant-like and that the reagent approaches from the less hindered side of the prevailing conformer. Here we estimated the ratio of the diastereoisomeric products **2** and **3** (Fig. 3), using a procedure similar to that used to study the oxidation of sulfides. Thus, approach of the nucleophile to **1** may take place more easily from the less hindered side of the carbonyl π -face. Rotamers **a** and **a'** will give **2** [Figs. 3(A) and 3(B)] as the predominant product ($x > y$). Rotamer **b** may give **2** and **3** in equal amounts [Fig. 3(C), $x = z$].

As shown in Table 1, the torsion angle ϕ in rotamer **a** is much smaller ($71–79^\circ$) than in rotamer **a'** ($92–96^\circ$). Hence it is reasonable to envisage a differing π -facial selection for the approach of the reagent in the cases of rotamers **a** and **a'**. In rotamer **a**, formation of a 5-member CH/π hydrogen bond is

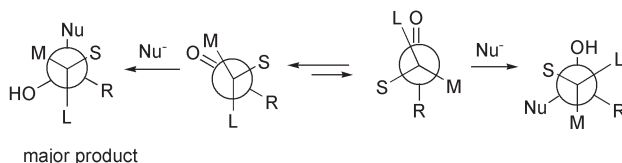
Table 2 Rotameric abundance (%) of alkyl 1-phenylethyl ketones $C_6H_5CHCH_3COR$ **1**

R	Rotamer a	Rotamer a'	Rotamer b
CH_3	95.9	–	4.1
C_2H_5	94.3	2.6	3.1
$i-C_3H_7$	90.2	8.4	1.4
$t-C_4H_9$	–	100.0	0.0

(a) Cram open-chain model



(b) Karabatsos model



(c) Felkin model

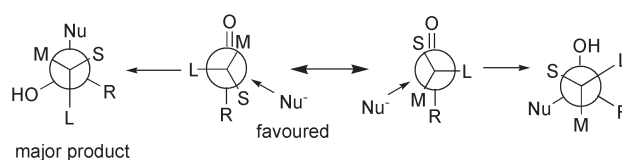
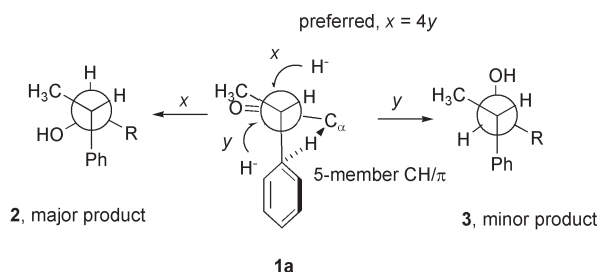
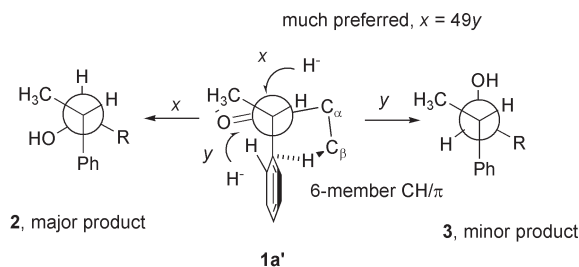


Fig. 2 Various models dealing with the nucleophilic addition to chiral acyclic carbonyl compounds. (a) Cram open-chain model. (b) Karabatsos model. (c) Felkin model.

(A)



(B)



(C)

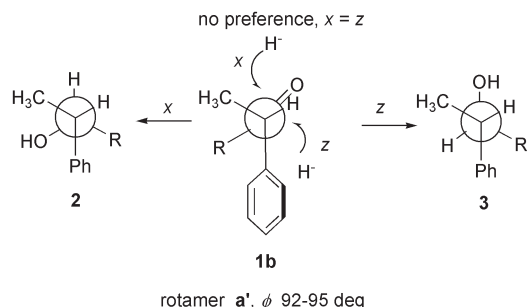


Fig. 3 Plausible explanations for the π -facial selectivity in the nucleophilic addition to alkyl 1-phenylethyl ketones.

possible, whereas in **a'** a 6-member CH/ π interaction should occur. In rotamer **a'**, the phenyl group must rotate to make an effective 6-member CH/ π bond. Consequently, one of the two ortho hydrogens orients itself toward the carbonyl π -face. The torsion angle α defined by C_{ortho}–C_{ipso}–C–C(=O) in rotamer **a'** is in fact found to be smaller (50–51°) than in rotamer **a** (55–56°). Accordingly, distances between H_{ortho} and the carbonyl group are shorter in rotamer **a'** than in rotamer **a**. Table 3 summarizes the data.

In rotamer **a'**, approach of the reagent from this side of the C=O π -face will be much disturbed. By assuming $x = 4y^{26}$ for rotamer **a** [Fig. 3(A)] and $x = 49y^{27}$ for rotamer **a'** [Fig. 3(B)], the ratio of the diastereomeric products **2:3** in the nucleophilic attack to **1** is predicted to be 3.7:1, 3.9:1, 4.3:1 and 49:1, respectively, for R = CH₃, C₂H₅, *i*-C₃H₇ and *t*-C₄H₉ (Table 4).

Felkin and coworkers reported that LiAlH₄ reduction of alkyl 1-phenylethyl ketones C₆H₅CHCH₂COR, **1**, gave diastereomeric alcohols in differing yields: **2:3** = 2.8:1, 3.2:1, 5.0:1 and 49:1, respectively, in the above order. Their results, together with those reported for similar reactions, are given in Table 5.^{28,29} Different data were reported, depending on the substrate, reagent and conditions of the reaction. According to our model, the correct structure of the major product can be predicted by a simple consideration of the equilibrium of the rotamers. When L = C₆H₅, a gradual increase of the product ratio **2:3** in the smaller alkyl homologues is followed by an abrupt jump at R = *t*-butyl. The ratio of the product alcohols does not obey this pattern, however, if L is a non-aromatic group such as cyclohexyl. This is understood since in the latter case the CH/ π interaction does not occur.

Table 3 Torsion angles defined by C_{ortho}–C_{ipso}–C–C(O) (α) and CH₃–C–C=O (ψ) in ° and distances $d_{\text{H}_{\text{ortho}}/\text{C}}$, $d_{\text{H}_{\text{ortho}}/\text{O}}$, $d_{\text{CH}/\pi}$ and $d_{\text{CH}/\text{O}}$ in Å

R	Rotamer	α	ψ	$d_{\text{H}_{\text{ortho}}/\text{C}}$ ^a	$d_{\text{H}_{\text{ortho}}/\text{O}}$ ^b	$d_{\text{CH}/\pi}$ ^c	$d_{\text{CH}/\text{O}}$ ^d
CH ₃	a	56	23	2.766	2.715	2.853	2.538
C ₂ H ₅	a	56	25	2.764	2.679	2.830	2.621
	a'	56	20	2.758	2.747	2.830	2.634
	a'	51	37	2.735	2.492	2.848	2.592
<i>i</i> -C ₃ H ₇	a	55	16	2.738	2.793	2.770	2.654
	a'	51	40	2.749	2.462	2.792	2.588
	a'	51	34	2.721	2.504	2.973	2.583
<i>t</i> -C ₄ H ₉	a'	50	36	2.725	2.476	2.910	2.565

^a Distance between H_{ortho} and carbonyl carbon atom. ^b Distance between H_{ortho} and carbonyl oxygen atom. ^c Distance between CH (α -CH for **a**, β -CH for **a'**) and C_{ipso}. ^d Distance between one of the three CHs in the benzylic methyl group and the carbonyl oxygen atom.

Table 4 Ratio of the diastereoisomeric products **2:3** in the nucleophilic addition to carbonyl compounds **1**

R	Calculated			Observed ^a
	2	3	2:3	
CH ₃	78.8 ^b	21.2 ^c	3.71	2.9
C ₂ H ₅	79.5 ^d	20.5 ^e	3.89	3.2
<i>i</i> -C ₃ H ₇	81.1 ^f	18.9 ^g	4.29	5
<i>t</i> -C ₄ H ₉	98 ^h	2 ⁱ	49.0	49

^a Ratio of the product secondary alcohols **2:3** in LiAlH₄ reduction of **1** (ether, 35°C). ^b From $95.9 \times 0.8 + 4.1 \times 0.5$. ^c From $95.9 \times 0.2 + 4.1 \times 0.5$. ^d From $94.3 \times 0.8 + 2.6 \times 0.98 + 3.1 \times 0.5$. ^e From $94.3 \times 0.2 + 2.6 \times 0.02 + 3.1 \times 0.5$. ^f From $90.2 \times 0.8 + 8.4 \times 0.98 + 1.4 \times 0.5$. ^g From $90.2 \times 0.2 + 8.4 \times 0.02 + 1.4 \times 0.5$. ^h From 100×0.98 . ⁱ From 100×0.02 .

Table 5 Diastereoisomer ratios of the alcohols produced by the LiAlH_4 and NaBH_4 reductions of chiral acyclic ketones LCHCH_3COR

R	L = C_6H_5			L = <i>cyclo</i> - C_6H_{11}		
	LiAlH_4		NaBH_4	LiAlH_4		NaBH_4
	$T = 35^\circ\text{C}^a$	$T = -43^\circ\text{C}^b$	$T = 50^\circ\text{C}^b$	$T = 35^\circ\text{C}^a$	$T = -43^\circ\text{C}^b$	$T = 50^\circ\text{C}^b$
CH_3	2.8 (2.5 ^c)	4.9	1.6	1.6 (1.4 ^c)	2.7	1.2 (1.7 ^d)
C_2H_5	3.2 (2.0 ^c)	5.5	2.0	2.0	3.8	1.6
<i>i</i> - C_3H_7	5.0	5.9	2.7	4.1	9.7	3.2
<i>t</i> - C_4H_9	49	216	7.3	1.6	1.5	3.5

^a Ethyl ether (Ref. 3). ^b Isopropanol (Ref. 28). ^c Ethyl ether (Ref. 1). ^d Aqueous methanol (Ref. 29).

Energetics of the transition structures of the hydride addition to alkyl 1-phenylethyl ketones

Next, we carried out *ab initio* calculations of the transition states of a model reaction. The geometries of the diastereomeric transition states ($\text{C}_6\text{H}_5\text{CHCH}_3\text{COR} + \text{LiH}$ with $\text{R} = \text{CH}_3$, C_2H_5 , *i*- C_3H_7 , *t*- C_4H_9) were optimized, at the MP2/6-31G(d) level, starting from the favoured conformation of **1**. Single-point calculations were carried out at the MP2/6-311G(d,p) level to estimate the Gibbs energy of the transition structures. Table 6 summarizes the results. Differences in the transition structures, leading to products **2** and **3**, show a similar tendency as the substituent effect in the product ratios estimated on the basis of the rotameric equilibrium. For instance, the difference in the Gibbs energies between TS1 and TS2 is 1.37 kcal mol⁻¹ for $\text{R} = \text{CH}_3$, whereas it is 4.13 kcal mol⁻¹ for $\text{R} = \text{t-C}_4\text{H}_9$.

Table 7 lists some of the geometrical parameters and the transition-state structures for $\text{R} = \text{CH}_3$ and *t*- C_4H_9 are given in Fig. 4. The transition-state geometry TS1 that leads to the predominant product **2** is not much different from the ground-state conformation. In the geometries, TS2, leading to the minor product **3**, on the contrary, torsion angles ϕ , ψ and α are twisted considerably to avoid unfavourable steric constraints. Notice that the CH/π and CH/O distances are very short in all the transition-state geometries. These results demonstrate that these weak hydrogen bonds play an important part in stabilizing the transition structures. The CH_3/O torsion angle ψ in the transition geometry TS1 leading to the major product is 23–33°. Consistent with this observation, the methyl group was reported to be close to $\text{C}=\text{O}$ in the most stable transition structure of nucleophilic reactions (LiH , NaH etc.) with propanal,^{8,23} 2-chloropropanal, 2-methoxypropanal, 2-*N,N*-dimethylpropanal,³⁰ 2-fluoropropanal,³¹ 2-silylpropanal and 2-trimethylsilylpropanal.³²

Table 6 Relative Gibbs energy (kcal mol⁻¹) of the transition states calculated at the MP2/6-311G(d,p)/MP2/6-31G(d) level of approximation for the model reaction $\text{C}_6\text{H}_5\text{CHCH}_3\text{COR} + \text{LiH}$. In parentheses is given the $\text{C}_6\text{H}_5\text{--C--R}$ torsion angle ϕ in °

R	Rotamer	TS1 ^a	TS2 ^b	Rotamer	TS3 ^a	TS4 ^b
CH_3	a ^c	0.00 (67)	1.37 (30)	b	2.63 (–82)	3.79 (–27)
C_2H_5	a	0.00 (69)	1.86 (29)	b	2.55 (–83)	3.46 (–26)
	a	1.41 (65)	3.33 (29)	b	6.70 (–78)	5.88 (–22)
	a'	1.44 (67)	5.04 (37)	b'	5.00 (–86)	6.74 (–32)
<i>i</i> - C_3H_7	a	0.00 (64)	1.36 (29)	b	5.45 (–78)	4.15 (–22)
	a'	0.51 (76)	5.07 (37)	b'	7.17 (–66)	7.72 (–28)
	a'	1.88 (70)	4.29 (38)	b'	3.69 (–90)	5.52 (–34)
<i>t</i> - C_4H_9	a'	0.00 (71)	4.13 (39)	b'	6.53 (–68)	6.85 (–29)

^a Transition structure leading to the major product **2**. ^b Transition structure leading to the minor product **3**. ^c Starting geometry.

Table 7 Torsion angles defined by $\text{C}_{\text{ortho}}\text{--C}_{\text{ipso}}\text{--C--C(O)}$ (α) and $\text{CH}_3\text{--C--C=O}$ (ψ) in ° and distances $d_{\text{H}_\text{O}/\text{C}}$, $d_{\text{H}_\text{O}/\text{O}}$, $d_{\text{CH}/\pi}$ and $d_{\text{CH}/\text{O}}$ in Å at the transition-state structures. TS1 and TS2 in each entry correspond, respectively, to the transition structures leading to **2** and **3**

R	Rotamer	TS	α	ψ	$d_{\text{H}_\text{O}/\text{C}}^a$	$d_{\text{H}_\text{O}/\text{O}}^b$	$d_{\text{CH}/\pi}^c$	$d_{\text{CH}/\text{O}}^d$
CH_3	a ^e	TS1	59	27	2.822	2.696	2.826	2.633
		TS2	73	–39	3.187	4.119	2.600	2.587
C_2H_5	a	TS1	59	28	2.825	2.688	2.751	2.633
		TS2	73	–40	3.176	4.111	2.599	2.583
	a	TS1	54	25	2.753	2.662	2.915	2.618
		TS2	66	–41	3.086	4.058	2.645	2.576
	a'	TS1	64	28	2.904	2.764	2.739	2.632
		TS2	82	–34	3.331	4.181	2.597	2.573
<i>i</i> - C_3H_7	a	TS1	54	23	2.762	2.696	2.807	2.607
		TS2	65	–41	3.069	4.072	2.612	2.566
	a'	TS1	56	33	2.812	2.595	2.569	2.625
		TS2	72	–35	3.193	4.072	2.568	2.527
	a'	TS1	58	29	2.819	2.639	2.733	2.611
		TS2	83	–33	3.351	4.188	2.569	2.561
<i>t</i> - C_4H_9	a'	TS1	58	29	2.836	2.659	2.599	2.599
		TS2	71	–33	3.194	4.048	2.473	2.497

^a Distance between H_{ortho} and carbonyl carbon atom. ^b Distance between H_{ortho} and carbonyl oxygen atom. ^c Distance between CH ($\alpha\text{-CH}$ for **a**, $\beta\text{-CH}$ for **a'**) and C_{ipso} . ^d Distance between one of the three CHs in the benzylic methyl group and the carbonyl oxygen atom. ^e Starting geometry.

Conclusions

Ab initio MO calculations of alkyl 1-phenylethyl ketones $\text{C}_6\text{H}_5\text{CHCH}_3\text{COR}$, **1**, demonstrated that rotamers with a $\text{R}/\text{C}_6\text{H}_5$ synclinal geometry preponderate in the conformational equilibrium. Rotamer **a** is more favourable than **a'** since the former is stabilized by 5-member CH/π intramolecular hydrogen bonds whereas the latter is stabilized by less effective 6-member CH/π bonds. Consequently, the population of rotamer **a** is more than 90% in every case, except for $\text{R} = \text{t-C}_4\text{H}_9$.

The ratio of the diastereoisomeric products **2** and **3** in the nucleophilic addition to **1** was estimated on the basis of the above ground-state rotamer distribution (a classical approach). This model resembles, formally, the Karabatsos model in that the benzylic methyl group is close to $\text{C}=\text{O}$ in the stable rotamer.³³ However, our hypothesis is founded on the basis of the conformational equilibrium estimated by high-level *ab initio* calculations. In spite of its simplicity, the model provides a plausible explanation for the effect of the alkyl substituent. We conclude that the conformational effect is most important for the π -facial diastereoselectivity.³⁴ The exceptional effect of the *t*-butyl substituent on the stereoselectivity (both in the oxidation of sulfides²⁵ and the hydride reduction of ketones^{3,35}) is not rationalized in terms of the so-called secondary orbital interactions.³⁶

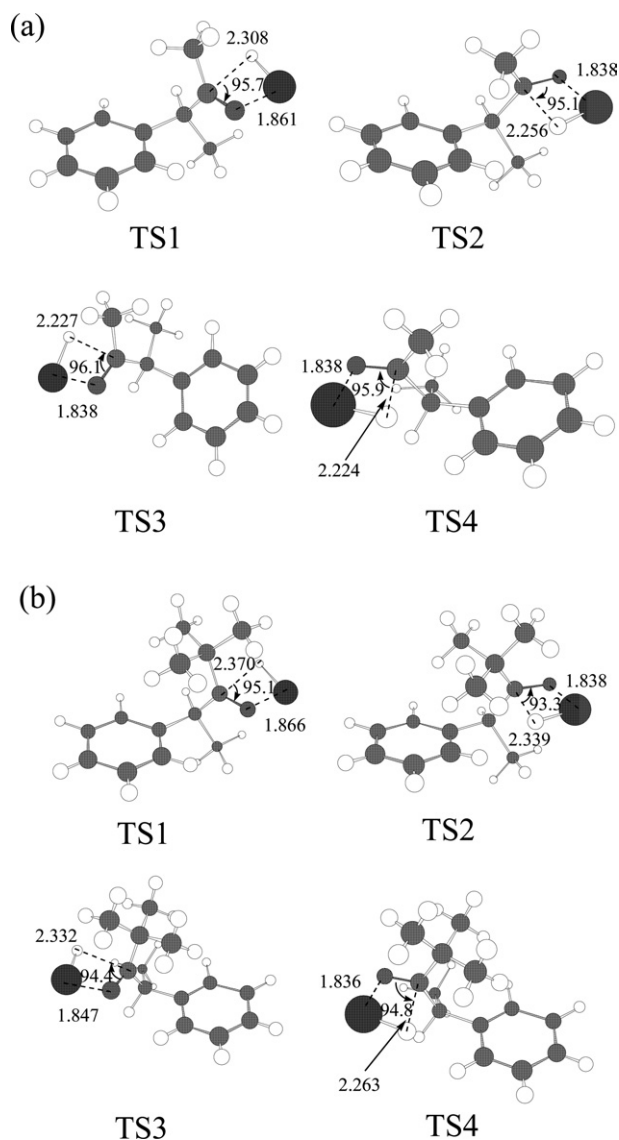


Fig. 4 Transition-state geometries calculated at the MP2/6-311G(d,p)//MP2/6-31G(d) level of approximation: (a) R = CH₃ and (b) R = *t*-C₄H₉. TS1 and TS3 are the transition-state structures leading to the predominant product 2, calculated starting from geometry a. TS2 and TS4 are the transition-state structures leading to the minor product 3, calculated starting from geometry b.

The Gibbs energy of the transition structures has also been calculated.³⁷ The result is consistent with the substituent effect in the product ratios estimated from the rotameric equilibrium. The transition-state geometries leading to the predominant product are similar to those of the ground-state conformation. In geometries leading to the minor product, the relevant torsion angles are significantly twisted relative to the ground-state conformations. In spite of this, short CH/π and CH/O distances are found in every case, suggesting that these weak hydrogen bonds are operating to stabilizing the otherwise unfavourable transition structures.

Acknowledgements

The authors thank the Institute for Non-linear Science and Applied Mathematics at Hiroshima University for the use of a NEC HSP, the Information Media Center at Hiroshima University for the use of a H9000 VR360, and the Research Center for Computational Science, Okazaki National Research Institutes, for the use of a Fujitsu VPP5000.

References

- 1 D. J. Cram and F. A. Abd Elhafez, *J. Am. Chem. Soc.*, 1952, **74**, 5828–5835.
- 2 J. W. Cornforth, R. H. Cornforth and K. K. Mathew, *J. Chem. Soc.*, 1959, 112–121.
- 3 M. Chérest, H. Felkin and N. Prudent, *Tetrahedron Lett.*, 1968, 2199–2204.
- 4 G. J. Karabatsos, *J. Am. Chem. Soc.*, 1967, **89**, 1367–1371.
- 5 E. L. Eliel, S. V. Frye, E. R. Hortelano, X. Chen and X. Bai, *Pure Appl. Chem.*, 1991, **63**, 1591–1598; M. T. Reetz, *Acc. Chem. Res.*, 1993, **26**, 462–468.
- 6 E. L. Eliel, S. H. Wilen and L. N. Mander, *Stereochemistry of Organic Compounds*, Wiley-Interscience, New York, 1994, pp. 876–880.
- 7 A. Mengel and O. Reiser, *Chem. Rev.*, 1999, **99**, 1191–1223.
- 8 G. Frenking, K. F. Köhler and M. T. Reetz, *Tetrahedron*, 1991, **47**, 8991–9004; G. Frenking, K. F. Köhler and M. T. Reetz, *Tetrahedron*, 1991, **47**, 9005–9018.
- 9 S. S. Wong and M. N. Paddon-Row, *J. Chem. Soc., Chem. Commun.*, 1991, 327–330.
- 10 M. Chérest, H. Felkin, P. Tacheau, J. Jacques and D. Varech, *J. Chem. Soc., Chem. Commun.*, 1977, 372–373.
- 11 M. J. Frisch, G. W. Trucks, H. B. Schlegel, G. E. Scuseria, M. A. Robb, J. R. Cheeseman, V. G. Zakrzewski, J. A. Montgomery, Jr., R. E. Stratmann, J. C. Burant, S. Dapprich, J. M. Millam, A. D. Daniels, K. N. Kudin, M. C. Strain, O. Farkas, J. Tomasi, V. Barone, M. Cossi, R. Cammi, B. Mennucci, C. Pomelli, C. Adamo, S. Clifford, J. Ochterski, G. A. Petersson, P. Y. Ayala, Q. Cui, K. Morokuma, D. K. Malick, A. D. Rabuck, K. Raghavachari, J. B. Foresman, J. Cioslowski, J. V. Ortiz, B. B. Stefanov, G. Liu, A. Liashenko, P. Piskorz, I. Komaromi, R. Gomperts, R. L. Martin, D. J. Fox, T. Keith, M. A. Al-Laham, C. Y. Peng, A. Nanayakkara, C. Gonzalez, M. Challacombe, P. M. W. Gill, B. Johnson, W. Chen, M. W. Wong, J. L. Andres, C. Gonzalez, M. Head-Gordon, E. S. Replogle and J. A. Pople, *Gaussian 98 (Revision A.4)*, Gaussian Inc., Pittsburgh, PA, USA, 1998.
- 12 O. Takahashi, K. Yasunaga, Y. Gondoh, Y. Kohno, K. Saito and M. Nishio, *Bull. Chem. Soc. Jpn.*, 2002, **75**, 1777–1783.
- 13 M. Nishio, M. Hirota and Y. Umezawa, *The CH/π Interaction. Evidence, Nature, and Consequences*, Wiley-VCH, New York, 1998. A comprehensive literature list for the CH/π interaction is available at <http://www.tim.hi-ho-ne.jp/dionisio>.
- 14 CH/π interactions in conformational issues: M. Nishio and M. Hirota, *Tetrahedron*, 1989, **45**, 7201–7245; B. W. Gung, Z. Zhu and R. A. Fouch, *J. Am. Chem. Soc.*, 1995, **117**, 1783–1788; Y. Umezawa, S. Tsuboyama, H. Takahashi, J. Uzawa and M. Nishio, *Tetrahedron*, 1999, **55**, 10047–10056; H. Suezawa, S. Ishihara, H. Takahashi, K. Saito, Y. Kohno and M. Nishio, *New J. Chem.*, 2003, **27**, 1609–1613.
- 15 Organic chemists often postulate this type of geometry.
- 16 S. Zushi, Y. Kodama, K. Nishihata, K. Umemura, M. Nishio, J. Uzawa and M. Hirota, *Bull. Chem. Soc. Jpn.*, 1980, **53**, 3631–3640.
- 17 In a previous study we calculated the conformational Gibbs energies of alkylbenzenes C₆H₅CH₂R, at differing levels of approximation. No appreciable difference has been found between the data obtained from the different levels of theory: O. Takahashi, K. Saito, Y. Kohno and M. Nishio, *Chem.-Eur. J.*, 2003, **9**, 756–762.
- 18 G. R. Desiraju and T. Steiner, *The Weak Hydrogen Bond in Structural Chemistry and Biology*, Oxford University Press, Oxford, 1999, ch. 2.
- 19 Conformation: H. Yoshida, I. Kaneko, H. Matsuura, Y. Ogawa and M. Tasumi, *Chem. Phys. Lett.*, 1992, **196**, 601–606; H. Yoshida, T. Tanaka and H. Matsuura, *Chem. Lett.*, 1996, 637–638; O. Takahashi, Y. Kohno, Y. Gondoh, K. Saito and M. Nishio, *Bull. Chem. Soc. Jpn.*, 2003, **76**, 369–374.
- 20 Ab initio MO calculation: J. J. Novoa and F. Mota, *Chem. Phys. Lett.*, 1997, **266**, 23–30; Y. Gu, T. Kar and S. Scheiner, *J. Am. Chem. Soc.*, 1999, **121**, 9411–9422.
- 21 M. Nishio, M. Hirota and Y. Umezawa, *The CH/π Interaction. Evidence, Nature, and Consequences*, Wiley-VCH, New York, 1998, pp. 66–67 and 84–85; H. Suezawa, T. Hashimoto, K. Tsuchinaga, T. Yoshida and T. Yuzuri, K. Sakakibara, M. Hirota, M. Nishio, *J. Chem. Soc., Perkin Trans. 2*, 2000, 1243–1249.
- 22 G. J. Karabatsos and N. Hsi, *J. Am. Chem. Soc.*, 1965, **87**, 2864–2870.
- 23 Y.-D. Wu and K. N. Houk, *J. Am. Chem. Soc.*, 1987, **109**, 908–910.

- 24 O. Takahashi, K. Saito, Y. Kohno, H. Suezawa, T. Yoshida, S. Ishihara and M. Nishio, *New J. Chem.*, 2003, **27**, 1639–1643.
- 25 K. Nishihata and M. Nishio, *Tetrahedron Lett.*, 1977, 1041–1044.
- 26 The assumption is reasonable in view of the experimental data reported for the reduction of bicyclic ketones: M. J. Brienne, D. Varech and J. Jacques, *Tetrahedron Lett.*, 1974, 1233–1236.
- 27 This assumption was arbitrarily made to obtain acceptable fit with the experimental data.
- 28 M. Chérest and N. Prudent, *Tetrahedron*, 1980, **36**, 1599–1606.
- 29 D. J. Cram and F. D. Greene, *J. Am. Chem. Soc.*, 1953, **75**, 6005–6010.
- 30 G. Frenking, K. F. Köhler and M. T. Reetz, *Tetrahedron*, 1993, **49**, 3971–3982; G. Frenking, K. F. Köhler and M. T. Reetz, *Tetrahedron*, 1993, **49**, 3983–3994.
- 31 S. S. Wong and M. N. Paddon-Row, *J. Chem. Soc., Perkin Trans. 2*, 1990, 456–458.
- 32 I. Fleming, D. A. Hrovat and W. T. Borden, *J. Chem. Soc., Perkin Trans. 2*, 2001, 331–338.
- 33 Perusal of data in the literature indicates that the group attributed to M (medium size) is almost invariably an aliphatic one (bearing CHs); see Table 1 in: A. Mengel and O. Reiser, *Chem. Rev.*, 1999, **99**, 1191 entitled *Around and Beyond Cram's Rule*. This suggests that the CH/O hydrogen bond is working in stabilizing the preferred conformation.
- 34 G. Frenking, K. F. Köhler and M. T. Reetz, *Tetrahedron*, 1994, **50**, 11197–11204. We concur with Frenking that the conformation of the substrate molecules is the dominant factor in determining the diastereofacial selectivity of nucleophilic reactions.
- 35 D. Varech and J. Jacques, *Tetrahedron Lett.*, 1973, 4443–4446.
- 36 For criticisms to the secondary orbital interaction in stereoselectivity, see: J. I. Garcia, J. A. Majoral and L. Salvatella, *Acc. Chem. Res.*, 2000, **33**, 658–664; M. Sodupe, R. Rios, V. Branchadell, T. Nicholas, A. Oliva and J. J. Dannenberg, *J. Am. Chem. Soc.*, 1997, **119**, 4232–4238; B. W. Gung, *Chem. Rev.*, 1999, **99**, 1377–1386; G. Ujaque, P. S. Lee, K. N. Houk, M. F. Hentemann and S. J. Danishefsky, *Chem.-Eur. J.*, 2002, **8**, 3423–3430.
- 37 In order to examine whether the result differs from method to method, we carried out calculations at different levels of theory. The difference in the potential energy barrier (TS2 vs. TS1) for R = CH₃ has been found to be insignificant: 1.68, 1.61 and 1.56 kcal mol⁻¹, respectively, at the MP2/6-311G(d,p)//MP2/6-311G(d), MP2/6-311G(d,p)//MP2/6-311G(d,p) and MP4/6-311G(d,p)//MP2/6-311G(d) levels of approximation. Note that the above values are the difference in the potential energy barrier and not the Gibbs energy difference as reported in Table 6. See also ref. 17.